CTuL41

Excitation mechanism of the upper $^1D_2$ and $^2P_0$ levels in Tm:Yb:BaY$_2$F$_8$ laser crystal

M. A. Noginov, M. Curley, P. Venkateswarlu, H. P. Jenssen,* *Center for Nonlinear Optics and Materials, Department of Physics, Alabama A&M University, P.O. Box 1268, Normal, Alabama 35762*

We quantitatively studied upconversion in Tm:Yb:BaY$_2$F$_8$ laser crystal, determined the excitation scheme for the upper $^1D_2$ and $^3P_0$ metastable levels, and showed the possibility of avalanche pumping at 706 nm.

The metastable levels $^3F_4$, $^3H_4$, and $^1G_4$ in Tm:YbBaY$_2$F$_8$ are populated via sequential energy transfer from Yb[1-4] (Fig. 1). As was implied by Trash and Johnson,[5] $^1D_2$ is populated due to Tm-Tm interaction ($^3F_4 \rightarrow {}^3H_6$, $^3F_3 \rightarrow {}^1D_2$) and $^3P_0$ (potential upper laser levels for UV operation[5]) is excited via $^2F_{5/2}$Yb – $^1D_2$Tm interaction (Fig. 1). However, small lifetime of $^3F_3$ and large energy mismatch for $^3F_3 - {}^3F_3$ upconversion[5] made the excitation scheme above questionable.

Exciting samples with different dopant concentrations via Yb ions, in the pumping density range ~0.1–1000 W/cm^2, we studied luminescence spectra of Tm and Yb at 250–2200 nm, the dependence of the $^2T_4$, $^2T_{5/2}$, $^3H_4$, $^3P_2$, $^1G_4$, $^1D_2$, and $^3P_0$ luminescence intensity on pumping intensity, and luminescence kinetics of the above levels. At intense square-pulsed excitation, Yb luminescence kinetics features a maximum in the beginning of the pumping pulse followed by a slow decay, Fig. 2, determined by efficient $^2F_{5/2}$Yb – $^3F_4$Tm upconversion. The same characteristic shape is recognized in kinetics of the levels $^1G_4$ and $^3P_0$ but not $^1D_2$.

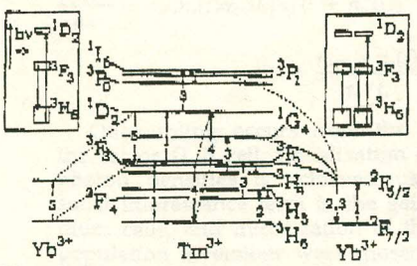

CTuL41 Fig. 1 Energy level diagram and main population processes in Tm:Yb:BaY$_2$F$_8$. 1) Absorption; 2) energy transfer from Yb to $^3H_4$ Tm; 3) energy transfer from Yb to excited Tm ions; 4) interaction of excited Tm ions; 5) cross relaxation; small arrows denote multiphonon relaxation.

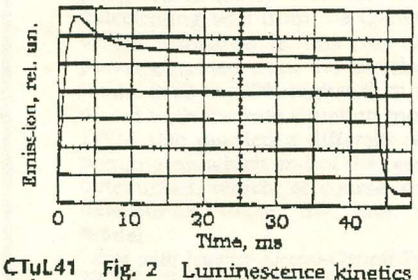

CTuL41 Fig. 2 Luminescence kinetics of $^2F_{5/2}$ Yb in Tm(0.5%):Yb(50%):BaY$_2$F$_8$ at strong direct excitation (~900 W/cm^2) with rectangular light pulse. The same characteristic shape was observed in the kinetics of $^1G_4$ and $^3P_0$, but not $^1D_2$.

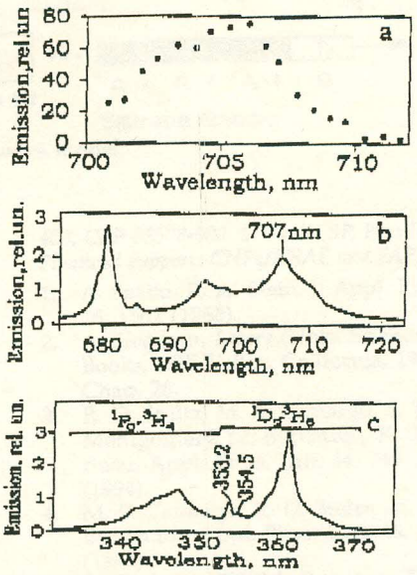

CTuL41 Fig. 3 a) Excitation spectrum of $^1D_2$ luminescence, b) luminescence spectrum of at the transition $^3F_3 - {}^3H_6$, and c) luminescence from the levels $^1D_2$ and $^3P_0$ at 340–370 nm.

We conclude that the levels $^3H_4$, $^1G_4$, and $^3P_0$ are populated via upconversion interaction of Yb and Tm; the level $^1D_2$ is excited via upconversion interaction of two $^3F_3$ states. Energy transfer parameters and optimization of ion concentrations are presented.

At red-light pumping, excitation spectrum of upconversion luminescence consists of one peak at ~706 nm (Fig. 3a). A 707-nm peak of the $^3F_3 \rightarrow {}^3H_6$ transition (Fig. 3b) and 353–354-nm lines of the $^1D_2 \rightarrow {}^3H_4$ transition (Fig. 3c) imply a resonance for excited-state absorption and upconversion. However, the sum of energies of the lower Stark level of $^3F_3$ (14586 cm^{-1})[6] and of 706-nm photon is more than 550 cm^{-1} larger than the energy of the highest known $^1D_2$ Stark level (28192 cm^{-1}).[6] Apparently in Tm:Yb:BaY$_2$F$_8$, excited-state absorption involves simultaneous absorption at 706 nm, radiationless relaxation of $^3F_3$ at ~ 707 nm, and excitation of $^1D_2$ at the transition starting from the bottom of the ground state 353–354 nm, (Fig. 1 left insert). Similarly, in the upconversion process, two $^3F_3$ Tm ions can relax to the ground state at ~707 nm and one of them get excited to $^1D_2$ at the transition starting from the bottom of $^3H_6$ (Fig. 1 right insert).

Under 706-nm excitation, upconversion efficiency increased with the increase of Yb concentration. We explain this effect with feeding $^3F_3$ via ($^2F_{5/2} \rightarrow {}^2F_{7/2}$, $^3F_4 \rightarrow {}^3F_2$, $^3F_3$) upconversion. In fact, excited-state absorption $^3F_3 \rightarrow {}^1D_2$, cross relaxation ($^1D_2 \rightarrow {}^3F_2$ (~>$^3F_3$), $^2F_{7/2} \rightarrow {}^2F_{5/2}$), energy transfer ($^2F_{5/2} \rightarrow {}^3H_5$ –> $^3F_4$), and $^2F_{5/2}$Yb – $^3F_4$Tm upconversion make a cycle of avalanche pumping (Fig. 1). At weak pumping, a 706-nm two-photon excitation of $^1D_2$ at has a potential advantage over excitation via Yb, which requires four photons.

*CREOL, *University of Central Florida, 12424 Research Parkway, Ste. 400, Orlando, Florida 32862*

1. Yu. P. Chukova, *Sovetskoe Radio*, Moskva, Moscow, 1980, p. 74 (in Russian).
2. B. M. Antipenko, *et al.*, Sov. J. Quantum Electron. 13, 558 (1983).
3. B. M. Antipenko, *et al.*, Opt. Spectrosk. 59, 626 (1985), in Russian.
4. X. X. Zxang, *et al.*, Phys. Rev. B, 51, p. 9298 (1995).
5. R. J. Trash, L. F. Johnson, J. Opt. Soc. Am. B, 11, 881 (1994).
6. H. P. Jenssen, *et al.*, MIT internal report, unpublished.

CTuL42

Traveling-wave model for a resonator containing a saturable absorber

Robert D. Stultz,* Marly B. Camargo,** Milton Birnbaum, *Center for Laser Studies, University of Southern California, DRB 17, University Park, Los Angeles, California 90089-1112*

The conventional rate equations for a passively Q-switched laser[1,2] are sufficient in cases where the cavity losses are relatively low. This is the usually the case with low-gain Er lasers.[3,4] For high-gain lasers, such as Nd:YAG or Er-doped fibers where outcoupling losses can be high, the simple rate equation model breaks down.[5] In addition, with the rate equation model, it is not possible to incorporate axial nonuniformities in the photon beam as in the case of a non-plane-parallel resonator, or nonuniformities in the population inversion as in an end-pumped configuration.

In our model, the resonator is divided into Ω_c cells, with $\Delta L = L_{opt}/\Omega_c$, where L_{opt} is the optical path length of resonator. For simplicity, the gain and absorber media are assumed to each occupy one-half of the resonator, and are divided into an equal number of cells. T_1, T_2, T_m are the transmittances of the empty cells and R_1, R_2 are the resonator mirror reflectivities. During the iteration, the gain, absorber population differences, and positive, negative-going photon densities are updated for each resonator cell. Outcoupling can be from either end of the resonator as shown in Fig. 1.

Equations for the photon densities and population differences were derived, based on the photon transport equation. The appropriate boundary conditions were applied at each end of the resonator. The following equations give the photon density (n_i^+ and n_i^-), and absorber population difference (n_a) rates for the ith cell in the saturable absorber. A similar set of equations were derived for the gain medium.

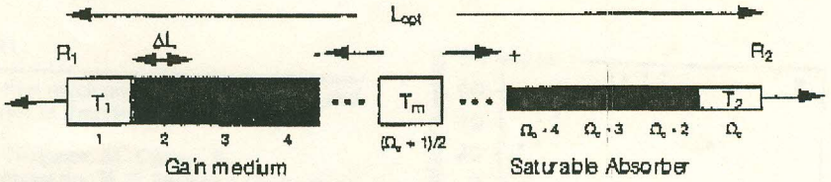

CTuL42 Fig. 1 Resonator for traveling-wave model.

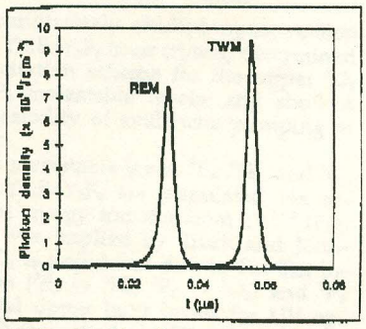

CTuL42 Fig. 2 Comparison of traveling-wave and rate equation models for case with 80% outcoupling and 70% initial saturable loss.

$$\frac{\Delta n_p^+(i)}{\Delta\tau} = (1 - \Delta L n_a(i)\sigma_a) n_p^+(i-1) - n_p^+(i)$$

$$\frac{\Delta n_p^-(i)}{\Delta\tau} = (1 - \Delta L n_a(i)\sigma_a) n_p^-(i+1) - n_p^-(i) \quad (1)$$

$$\frac{\Delta n_a(i)}{\Delta\tau} = -p_a n_a(i)\sigma_a \Delta L [n_p^+(i+n_p^-(i)] + \frac{n_{aT} - n_a(i)}{\tau_a / t_c} \quad (2)$$

Outcoupling occurs from the either the 1st or Ω_cth cell. Initialization of the photon densities is achieved using a small fluorescence term in the gain medium cells, and initialization of the cell population inversions were chosen such that the net round-trip gain was equal to the total initial saturable and nonsaturable losses.

The model is run using MATLAB on a MacIntosh Quadra 800. For low outcoupling and nonsaturable losses, the traveling-wave model (TWM) agrees exactly with the rate equation model (REM). Figure 2 compares simulated pulses from both models for a case with high outcoupling losses (80%). With the TWM, the outcoupling was from the Q-switch side of the resonator. In this case the peak power obtained from the traveling-wave model is about 20% higher than that predicted with the rate equation model. The TWM also predicts a different result depending on which end of the resonator is outcoupled, which, of course, cannot be determined using the rate equation model.

*Also with Hughes Electro-Optical Systems, 2000 E. El Segundo Blvd., El Segundo, California 90245-0902
**Present address: Instituto de Pesquisas Energéticas e Nucleares-MMO, Travessa R, 400, CEP 05508-900, S. Paulo, SP, Brazil.
Financial support: CNPq/RHAE and FAPESP.

1. A. Szabo, R. A. Stein, J. Appl. Phys. 36, 1562 (1965).
2. A. Siegman, *Lasers* (Univ. Science Books, Mill Valley, California, 1986), Chap. 26.
3. R. D. Stultz, M. B. Camargo, S. T. Montgomery, M. Birnbaum, K. Spariosu, Appl. Phys. Lett. 64, 948 (1994).
4. M. B. Camargo, R. D. Stultz, M. Birnbaum, Appl. Phys. Lett. 66, 2940 (1995).
5. D. H. Stone, IEEE J. Quantum Electron 28, 1970 (1992).

CTuL43

Pump-probe measurement of the upconversion gain in Tm^{3+}:YBF

David J. Simkin, Jianan Wang, Hans P. Jenssen,* *Department of Chemistry, McGill University, Montreal, Quebec, Canada H3A 1K6*

Interest in obtaining solid-state blue and green lasers that can be pumped with available red or near-infrared semiconductor laser diodes has stimulated research activity in upconversion materials. Upconversion pumped laser emission has been previously reported for Tm^{3+}:Y_2BaF_8,[1] however, there have been no studies to date on the upconversion gain reported for this material. Previous pump-probe gain measurements performed on Tm^{3+}:YLF[2] revealed several new features of interest that were not evident from prior spectroscopic and laser cavity experiments, so similar measurements were undertaken for Tm^{3+}:Y_2BaF_8 and are reported here.

The experimental arrangement used was the same as that previously reported in Ref. 2. The pump source was at 628 nm from a dye laser operating with

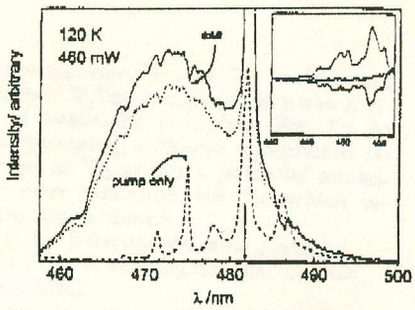

CTuL43 Fig. 1 Upconversion gain spectrum, $I_{pump+probe} - I_{pump}$ (solid line) compared with I_{probe} (dotted line), and I pump (dashed line), of Tm^{3+}:Y_2BaF_8 at 120 K for a pump power 460 mW and pump wavelength of 628 nm. Inset shows loss due to excited-state absorption in the $^1D_2 \rightarrow {}^3F_4$ transition region of the spectrum.

DCM. We specifically probed the $^1G_4 \rightarrow {}^3H_4$ transition at 482 nm. Because of the broad amplified spontaneous emission present in the wings of the probe laser pulses, relatively large spectral regions could be probed simultaneously. As in Ref. 2, we recorded spectra with pump plus probe, probe only, and pump only, and display the gain spectrum by comparing $I_{(pump+probe)} - I_{pump}$ with I_{probe}. Figure 1 shows such an upconversion gain spectrum at 120 K for a pump wavelength of 628 nm and a probe wavelength centered at 482 nm. We notice that there is a broad gain bandwidth ranging from 460 nm to 490 nm. This observation is in sharp contrast to the results for Tm^{3+}:YLF, in which case the gain was restricted to the narrow emission lines.

We obtained numerical results for the gain at three different probe wavelength from the areas of $[I_{(pump+probe)} - I_{pump}]/I_{probe}$. These values are given in Table 1. We also include the temperature dependence of the gain of the 482.9-nm emission line, which exhibits a curious maximum at some temperature near 160 K, before decreasing to unity (no gain or loss) at higher temperatures (c.a. 200 K). This unusual temperature behavior, and the broad-band gain exhibited over the range of 460–490 nm, may both result from stimulated emission from thermally populated higher Stark levels at higher temperatures. Eventually the thermal

CTuL43 Table 1 Measured Gain for Three Emission Lines in the $^1G_4 \rightarrow {}^3H_4$ Manifold of Tm^{3+}:Y_2BaF_8.

Probe λ /nm	Pump power /mW @ 628 nm	T /K	Gain ratio	α /cm^{-1}
475.0	400	11.9	1.17±.04	0.31±.07
482.9	460	11.9	1.30±.04	0.52±.06
	450	100.0	1.05±.03	0.10±.07
	450	160	1.40±.04	0.67±.06
	450	200	1.01±.03	0.02±.06
486.0	400	11.9	1.28±.04	0.49±.08

Tuesday Posters